1988

Dynamically Loaded Journal Bearings: Finite Volume Method Analysis

A. T. Prata
Federal University of Santa Caterina

R. T. S. S. Ferriera
Federal University of Santa Caterina

D. E. B. Mile
Empressa Brasileira de Compressores S/A-Embraco

M. G. D. Bortoli
Empressa Brasileira de Compressores S/A-Embraco

DYNAMICALLY LOADED JOURNAL BEARINGS:
FINITE VOLUME METHOD ANALYSIS

A. T. Prata, R. T. S. Ferreira
Department of Mechanical Engineering
Federal University of Santa Catarina
Cx.P. 476 - 88049 Florianópolis, SC - Brazil

D. E. B. Lilie and M. G. D. Bortoli
Empresa Brasileira de Compressores S/A - EMBRACO
Cx.P. D-27 - 89200 Joinville, SC - Brazil

ABSTRACT

This paper presents a numerical formulation for the analysis of journal bearings under dynamically loaded conditions. The solution of the Reynolds equation is determined using a control volume method, which allows mass conservation of the oil film to be always satisfied regardless the number of grid points used in the domain discretization. Use was made of nonorthogonal boundary fitted coordinates to accurately determine the shape of the cavitation boundary. The inclusion of cavitation turned the problem into a nonlinear free boundary value problem, and the solution methodology is described in detail. Results are presented in order to show the potencialities of the method. In the example chosen the bearing experiences a load that is suddenly increased in magnitude, and, after equilibrium has been reached, the load is brought back to its initial value. For this situation the journal describes a damped oscillatory motion. When cavitation is not considered, and, instead, the lubricant film extends from zero to Π (half Sommerfeld condition) the oscillation is less damped. The formulation have demonstrated to be effective and general.

NOMENCLATURE

c radial clearance
h film thickness, $= c(1+\varepsilon\cos\theta)$
L bearing length
p dimensionless pressure, equation (2)
p^* pressure
R bearing radius
t dimensionless time, equation (2)
t^* time
W load acting on the bearing
w journal angular rotation
w_L dimensionless speed corresponding to w_L^*, equation (2)
w_L^* angular rotation speed of load
y dimensionless coordinate corresponding to y^*, equation (2)
y^* axial distance measured from bearing midplane

α shape of the cavitation, boundary, function of y
Δ dimensionless load acting on the bearing, $= Wc^2/\mu w R^3 L$
Δt dimensionless time interval
ε clearance to eccentricity ratio
$\dot{\varepsilon}$ dimensionless time derivative of ε, $= d\varepsilon/dt$
η dimensionless angular coordinate, $= \theta/(\Pi+\alpha)$
θ angular coordinate measured from position of maximum clearance
μ lubricant viscosity
Ψ attitude angle
$\dot{\Psi}$ dimensionless time derivative of Ψ, $= d\Psi/dt$

INTRODUCTION

There are several situations in engineering where journal bearings are submitted to static loads. However, in most industrial applications it is a requirement that journal bearings be designed taking into account the transient behavior of the load acting on the bearings. In reciprocating compressors for example, the load variation is so intense that precludes any analysis based on a steady state regime.

In this regard, over the years attention have been directed to study journal bearings under dynamically loaded conditions. For a review of earliest works reference should be made to the papers by Burwell [1] and Milne [2]. In the sixties the mobility method devised by Booker [3-5], had a great impact on the analysis of dynamically loaded journal bearings. This method is still used very effectively nowadays despite its limitation to ideal bearings, i.e., bearings having circumferential symmetry and straight profiles along its axis. More recently the finite element [6-7] and the finite difference methods [8] have been applied to more general situations.

In the present work a numerical formulation for the analysis of journal bearings under dynamically loaded conditions is presented. The solution of the Reynolds equation is obtained using a control volume method. This method allows mass conservation of the oil film to be always satisfied, regardless the number of control volumes used in the domain discretization. Prior to the application of the numerical method, the Reynolds equation is written in nonorthogonal coordinates which fitted the boundary of the solution domain. Use of boundary fitted coordinates allowed the shape of the cavitation boundary to be accurately determined. The inclusion of cavitation turns the problem into a nonlinear free boundary value problem not easily solved. Recently, a cavitation algorithm was proposed by Elrod [9] and was, apparently well received by the scientific community [10-11]. Although Elrod's algorithm allows the cavitation boundary to be determined automatically during the solution of Reynolds equation, the shape of this boundary is obtained by interpolation along the grid points. The methodology to be presented is free from this limitation because the nonorthogonal coordinates adapt to the cavitation boundary. In what follows details of this methodology are described.

ANALYSIS

Problem Formulation. The Reynolds equation for journal bearings under dynamically loaded conditions can be written in cylindrical coordinates as [12].

$$\frac{1}{R^2}\frac{\partial}{\partial\theta}\left(h^3\frac{\partial p^*}{\partial\theta}\right) + \frac{\partial}{\partial y^*}\left(h^3\frac{\partial p^*}{\partial y^*}\right) = 6\mu\left[(w-2w_L^* - \frac{d\Psi}{dt^*})\frac{\partial h}{\partial\theta} + 2c\frac{d\varepsilon}{dt}\cos\theta\right] \quad (1)$$

where all quantities are defined according to the nomenclature.

Making use of the following dimensionless quantities,

$$p = p^* c^2(1+\varepsilon\cos\theta)^{3/2}/6\mu w R^2\ ,\ y = y^*/R\ ,\ t = wt^* \text{ and } w_L = w_L^*/w \quad (2)$$

equation (1) becomes,

$$\partial^2 p/\partial y^2 + \partial^2 p/\partial\theta^2 = A(\theta)\dot{\varepsilon} + B(\theta)\dot{\Psi} + C(\theta)p + D(\theta) \quad (3)$$

where $\dot{\varepsilon}$ and $\dot{\Psi}$ are the dimensionless time derivatives of ε and Ψ, respectively, and

$$A(\theta) = 2\cos\theta/(1+\varepsilon\cos\theta)^{3/2}$$
$$B(\theta) = 2\varepsilon\,\mathrm{sen}\theta/(1+\varepsilon\cos\theta)^{3/2}$$
$$C(\theta) = (-3/4)(2\varepsilon\cos\theta+\varepsilon^2\cos^2\theta + \varepsilon^2\cos2\theta)/(1+\varepsilon\cos\theta)^2$$
$$D(\theta) = (2w_L-1)(\varepsilon\,\mathrm{sen}\theta)/(1+\varepsilon\cos\theta)^{3/2}$$

Equation (3) is the form of the Reynolds equation which is suitable for the present analysis. From equation (3) the pressure distribution can be determined as a function of t, provided that w_L, ε, $\dot{\varepsilon}$, and $\dot{\Psi}$ are known. Commonly, the load angular rotation w_L is prescribed a priori, whereas ε, $\dot{\varepsilon}$ and $\dot{\Psi}$ should be obtained in connection with the load instantaneous value. This is so because the values of ε, $\dot{\varepsilon}$ and $\dot{\Psi}$ at a given time, should be such that furnish a pressure field that, when integrated, yields the load at that time. Therefore, to determine p, the values of ε, $\dot{\varepsilon}$ and $\dot{\Psi}$ should be given, but, in turn, ε, $\dot{\varepsilon}$ and $\dot{\Psi}$ depend upon p. This link between pressure and ε, $\dot{\varepsilon}$ and $\dot{\Psi}$ makes the solution of Reynolds equation only possible by iteration, except for very simplified situations. Details about this iterative procedure will be discussed later.

In order to complete the problem formulation, attention will now be directed to the boundary conditions. At the boundaries $\theta=0$, and $y=L/R$, where L and R are, respectively, the bearing length and the shaft radius, the pressure is set equal to zero. Furthermore, making use of the axial symmetry of the problem, $\partial p/\partial y=0$ along a plane that passes through the shaft center, that is, at $y=0$; in this regard, for the present investigation only half of the bearing is represented in the solution domain.

At this point only the boundary condition at the cavitation boundary is left to be discussed. For the present work, use will be made of the Reynolds free-surface condition |9-13|. Several authors have investigated the validity of this boundary condition |8,13-16|. In this regard, the analysis performed by Savage |13| deserves a special mention. In his work Savage shows using stability arguments that the Reynolds free-surface condition have physical grounds for situations where the pressure due to surface tension can be neglected. Surface tension effects can be ignored for capillary numbers $\beta \ll 1$, in which $\beta = \sigma c/\mu$, and σ is the surface tension. The condition $\beta \ll 1$, is normally satisfied for the type of applications in consideration here.

Making use of the Reynolds conditions at the cavitation boundary, that is, at $\theta=\Pi+\alpha(y)$, the pressure field should satisfy the following requirements, $p=\partial p/\partial\theta=0$. Two facts should be noted about the location of the cavitation boundary; first is that it is a function of y, which means that this boundary does not lie along a line of constant θ, and second, $\alpha(y)$ is not known a priori and should be calculated as the solution of the pressure field proceeds iteractively.

The main difficulty associated to the formulation just presented, is related to the calculation of $\alpha(y)$. To deal with this class of nonlinear free boundary value problem, the solution domain is transformed into a more tractable shape using a new coordinate, η , in the θ-direction defined as $\eta=\theta/|\Pi+\alpha(y)|$.

The key result of the transformation is that the η coordinate extends from zero to one for all values of y. Now, in the new coordinate system, the cavitation boundary lies along a line of constant η, that is, $\eta=1$. Therefore, the system η,y just proposed fits the boundaries of the solution domain.

Equation (3) written is the new system becomes,

$$\partial^2p/\partial y^2 + |1/(\Pi+\alpha)^2|\partial^2p/\partial\eta^2 = A|\eta(\Pi+\alpha)|\dot{\varepsilon} + B|\eta(\Pi+\alpha)|\dot{\Psi} + C|\eta(\Pi+\alpha)|p + D|\eta(\Pi+\alpha)| \qquad (5)$$

where, for simplicity, the indication that $\alpha = \alpha(y)$ was omitted.

Since $\eta = \eta(y)$, the η,y coordinates are nonorthogonal, and in writing equation (5) there should be some extra terms related to $\partial\eta/\partial y$. In the present work those terms are neglected. This approximation is in the same spirit of the local similarity model commonly used in the analysis of boundary layer flows, and is in accordance with the type of problem treated here.

The boundary conditions in the η direction now becomes $p=0$ at $\eta=0$, and $p=\partial p/\partial\eta=0$ at $\eta=1$. In the y direction the boundary conditions remain unaltered.

At this point the differential equation (5) is ready to be integrated. Details of this integration will be discussed next.

Discretization Equations. The first step towards the numerical integration is to divide the solution domain in small nonoverlaping control volumes; the solution domain is the region bounded by the lines of $y=0$, $y=L/R$, $\eta=0$ and $\eta=1$.

Next, equation (5) is integrated over each one of the control volumes. To perform this integration the pressure is assumed to prevail over the whole control volume, and the derivatives of pressure with respect to y and η are determined using a central difference approximation. From the integration of the differential equation results an algebraic equation for each control volume; these algebraic equations have the following form,

$$a_P p_P = a_0 p_0 + a_L p_L + a_N p_N + a_S p_S + S \qquad (6)$$

in which

$$a_0 = \Delta y/|(\Pi+\alpha)^2\delta\eta_o|, \quad a_L = \Delta y/|(\Pi+\alpha)^2\delta\eta_L| , \quad a_N = \Delta\eta/\delta y_N$$

$$a_S = \Delta\eta/\delta y_S , \quad a_P = a_0+a_L+a_N+a_S+ C|(\Pi+\alpha)\eta|\Delta z\ \Delta\eta \qquad (7)$$

$$S = -\{A|(\Pi+\alpha)\eta|\dot{\varepsilon} + B|(\Pi+\alpha)\eta|\dot{\Psi} + D|(\Pi+\alpha)\ \eta|\}\ \Delta y\ \Delta\eta$$

where the nomenclature associated to equation (6) is explained in Fig. 1. Equation (6) yields the pressure for the grid point P in terms of its four neighbors , p_O , p_L, p_N and p_S. As explained earlier, the pressure p_P prevails over the entire control volume depicted in Fig. 1.

For each control volume in the solution domain there is an algebraic equation of the type of equation (6). The set of all algebraic equations together with the boundary conditions is solved iteratively using the line-by-line method |17-18|. This method which is a combination of the Tri-Diagonal Matrix Algorithm and the Gauss-Seidel method have been extensively used to solve heat transfer problems (see for example |19|).

The pressure field obtained from the solution of the algebraic equations should be such that precisely balance the load acting on the bearing. Therefore, the pressure field should satisfy the following equations,

$$\Delta \cos\Psi = (Wc^2/\mu wR^3L)\cos\Psi = -6(R/L)\int_0^{L/R}\int_0^1 \frac{(\Pi+\alpha)\cos\theta}{(1+\varepsilon\cos\theta)^{32}}\, p\, d\eta dy$$

$$\Delta \,\mathrm{sen}\Psi = (Wc^2/\mu wR^3L)\mathrm{sen}\Psi = 6(R/L)\int_0^{L/R}\int_0^1 \frac{(\Pi+\alpha)\,\mathrm{sen}\theta}{(1+\varepsilon\cos\theta)^{32}}\, p\, d\eta dy \qquad (8)$$

where the dimensionless load $\Delta(= Wc^2/\mu wR^3L)$ is the Sommerfeld number.

Equations (8) will now be used to obtain $\dot\varepsilon$ and $\dot\Psi$, which are quantities required for the calculation of S in equation (7). To this extent equations (8) are discretized and the pressure p_P at each control volume is substituted by p_P given in equation (6). After some rearrangements it is obtained,

$$\Delta \cos\Psi = - I_1 + I_2\,\dot\varepsilon + I_3\,\dot\Psi \qquad (9a)$$

$$\Delta\,\mathrm{sen}\Psi = I_4 - I_5\,\dot\varepsilon - I_6\,\dot\Psi \qquad (9b)$$

where I_1, I_2,..., I_6 are integrals over the solution domain, and depend upon the pressure field |20|.

Isolating Ψ from equation (9b) and substituting the resulting expression into equation (9a) yields

$$\dot\varepsilon = \frac{\Delta|(I_6/I_3)\cos\Psi + \mathrm{sen}\Psi| - (I_4 - I_6I_1/I_3)}{I_2I_6/I_3 - I_5} \qquad (10)$$

knowing $\dot\varepsilon$, equation (9b) can be used to determine $\dot\Psi$ as

$$\dot\Psi = (I_4 - \Delta\mathrm{sen}\Psi + I_5\dot\varepsilon)/I_6 \qquad (11)$$

Equations (10) and (11) are the two equations employed to correct $\dot\varepsilon$ and $\dot\Psi$ as will be explained in the solution methodology. Except for the cavitation boundary, the problem formulation has now been completed. The determination of the cavitation boundary is obtained by imposing continuity of the liquid film for each control volume adjacent to the line of η=1. A mass balance at those control volumes yields expressions for $\alpha = \alpha(y)$. Those expressions are then used to update the values of α for each control volume from the pressure distribution. More details about the calculation of α can be found in |20,21].

SOLUTION METHODOLOGY

The first step in determining the numerical solution is to guess a pressure field, and a distribution for $\alpha(y)$, α=0 for example. At t=0, the shaft position should be also known through ε and Ψ, as well as the load Δ and its speed of angular rotation w_L. Next, the set of algebraic equations given by (6) is solved for the first iteration. As was discussed earlier, the values of $\dot{\varepsilon}$ and $\dot{\Psi}$ are not known at this point and should be guessed; here they were both made equal to zero. The pressure field calculated for this first iteration after being integrated does not yield the load Δ as is already expected. The following step in the solution methodology is to correct the $\dot{\varepsilon}$ and $\dot{\Psi}$ values. To this end equations (10) and (11) are activated. With those new values of $\dot{\varepsilon}$ and $\dot{\Psi}$ the pressure equation (6) is solved once more to update the pressure field. The new pressure field is next used to correct $\dot{\varepsilon}$ and $\dot{\Psi}$ once more which is again employed to recalculate p. This procedure is repeated until the values of p, $\dot{\varepsilon}$ and $\dot{\Psi}$ yield the specified load Δ.

Now, having obtained the converged pressure field for the first time step, the solution is ready to advance in time. The shaft location for the next time is determined from the following equations,

$$\varepsilon_{t+\Delta t} = \varepsilon_t + \dot{\varepsilon}\Delta t \quad \text{and} \quad \Psi_{t+\Delta t} = \Psi_t + \dot{\Psi}\Delta t \tag{12}$$

With the new values of ε and Ψ the procedure discribed in the previous paragraphs is repeated. Whenever a new pressure field is determined the shape of the cavitation boudary is also updated.

Based on the methodology just described, a computer program was written. The input variables of the program are: ε and Ψ values at t=0; dimensionless load acting on the bearing, Δ ; dimensionless angular rotation speed of load, w_L ; bearing aspect ratio, y/R ; dimensionless time interval, Δt. As output the program gives the journal locus as function of time.

It was observed that, as the solution proceeds marching on time, and the available values of $\dot{\varepsilon}$ and $\dot{\Psi}$ from the previous time is used to calculate a new pressure field, few iterations are necessary to update $\dot{\varepsilon}$ and $\dot{\Psi}$. This is especially true for small time intervals. For a typical time step, iterations were performed to correct the cavitation boundary $\alpha(y)$, and the time derivaties $\dot{\varepsilon}$ and $\dot{\Psi}$. Due to the presence of highly nonlinear terms, underrelaxation was employed to avoid divergence.

APPLICATION

The solution methodology just described will now be applied to a specific problem. In the example chosen the bearing experiences a load that is suddenly increased in magnitude, and, after equilibrium has been reached, the load is brought back to its initial value. The reason for choosing this problem is because the bearing experiences different values of $\dot{\varepsilon}$ and $\dot{\Psi}$, and in this regard, the numerical scheme can be properly tested.

For the situation under consideration, the bearing aspect ratio is L/R=2, and the journal initial location is that corresponding to ε=0.20 and Ψ=74° for a dimensionless load of Δ=0.6.

At t=0 the load is increased by 20% of its initial value. The bearing is not capable of sustain this augmented load and the shaft is forced to a new position. In order to show the variations of ε with time, Fig. 2 was prepared. In this figure, the clearance to eccentricity ratio ε is placed on the ordinate and the time t on the abscissa. Two curves are shown in Fig. 2, the solid curve is for the situation in which cavitation is considered, whereas, when cavitation is not considered, and, instead, the lubricant film extends from zero to Π(half Sommerfeld condition), the journal locus with time is described by the dashed line.

The first result to be extracted from Fig. 2 is that the shaft seeks its new equilibrium position in a damped oscillatory motion; when cavitation is considered, the oscillation is more damped. As seen from the figure, when the load is augmented, the shaft moves towards the bearing, increasing ε; however, due to its inertia, the shaft overshoots its equilibrium position and is forced back to a lower ε because the hydrodynamic forces resulting from high ε overcomes the load. Again, as it moves apart from the bearing, the shaft overshoots the equilibrium position; this time because the load is larger than the hydrodynamic forces. This oscillation is damped as time passes until the shaft reach its equilibrium position. For the case investigated in Fig. 2 the equilibrium was reached for t $\simeq$ 20. Since the time step was Δt=0.01, it took 2000 iterations to reach equilibrium.

For both situations described in Fig. 2 the oscillation frequency of the journal as it seeks equilibrium is constant and around 1/8 of the journal rotation frequency. This result is in agreement with those obtained through considerations about hydrodynamic stability of the oil film as discussed in |22|, chapter 8.

After equilibrium was reached as described in Fig. 2 the load was decreased by 20% assuming its original value at t=0. As expected, the shaft returned to its original position, that is, ε=0.20 and Ψ=74°. The results corresponding to this situation are presented in Fig. 3 . This figure resembles Fig. 2 in all aspects, except that the oscillating amplitude is a little higher in Fig. 3 than in Fig. 2.
The complete cycle will now be presented in a single curve. To this end Fig. 4 was prepared. This figure also show the shaft orbit for two situations, with and without cavitation of the lubricant film.

Additional tests of the computer program |23| have demonstrated that the formulation described here is effective and general.

CONCLUSIONS

A numerical formulation for journal bearings submitted to dynamic loads is introduced and discussed. The methodology presented makes use of finite volumes, and nonorthogonal boundary fitted coordinates. A cavitation algorithm is incorporated into the numerical scheme which allowed the cavitation boundary to be automatically determined as the solution proceeds iteratively marching on time.

As an application of the solution methodology, an example was chosen so that the bearing experienced a load that was suddenly increased in magnitude, and, after equilibrium was reached, the load magnitude was decreased to its initial value. In this example the shaft experienced a damped oscillatory motion while it sought equilibrium. The orbit described by the shaft was presented in graphic form for two situations: when cavitation was considered, and when cavitation was not considered, and, instead, the lubricant film extended from zero to Π. In presence of cavitation, the oscillation of the shaft is more damped.

Since the numerical solution was obtained using the full Reynolds equation, the methodology has demonstrated to be general and versatile. Analysis of nonideal bearing configurations with the present methodology can be performed with no additional complications.

ACKNOWLEDGMENTS

The present work is part of a technical-scientific agreement between Federal University of Santa Catarina and EMBRACO. The authors acknowledge both institutions for the financial support, and for the permission to release the information contained herein.

REFERENCES

|1| J. T. Burwell, "The Calculated Performance of Dynamically Loaded Sleeve Bearings", ASME Journal of Applied Mechanics, Vol. 73, pp. 393-404, 1951.

|2| A. A. Milne, "Theoretical Studies of the Performance of Dynamically Loaded Journal Bearings", N.E.L. Report Nº 70, of the National Engineering Laboratory of Glasgow, December 1962.

|3| J. F. Booker, "Dynamically Loaded Journal Bearings: Mobility Method of Solution", ASME Journal of Basic Engineering, Vol. 87, pp. 537-546, 1965.

|4| J. F. Booker, "Dynamically Loaded Journal Bearings: Maximum Film Pressure", ASME Journal of Lubrication Technology, Vol. 91, pp. 534-543, 1969.

|5| J. F. Booker, "Dynamically Loaded Journal Bearings: Numerical Application of the Mobility Method", ASME Journal of Lubrication Technology, Vol. 93, pp. 168-176, 1971.

|6| P. K. Goenka, "Dynamically Loaded Journal Bearings: Finite Element Method Analysis, " ASME Journal of Tribology, Vol. 106, pp 429-439, 1984.

|7| G. A. La Bouff and J. F. Booker, "Dynamically Loaded Journal Bearings: A Finite Element Treatment for Rigid and Elastic Surfaces, "ASME Journal of Tribology, Vol. 107, pp. 505-515, 1985.

|8| D. E. Brewe, "Theoretical Modeling of the Vapor Cavitation in Dynamically Loaded Journal Bearings," ASME Journal of Tribology, Vol. 108, pp. 628-638, 1986.

|9| H. G. Elrod, "A Cavitation Algorithm," ASME Journal of Lubrication Technology, Vol. 103, pp. 350-354, 1981.

|10| J. F. Booker, "Discussion of the paper by H. C. Elrod," ASME Journal of Lubrication Technology, Vol. 103, p. 354, 1981.

|11| A. O. Lebeck, "Discussion of the paper by H. C. Elrod," ASME Journal of Lubrication Technology, Vol. 103, p.354, 1981.

|12| A. Cameron, "The Principles of Lubrication," Longmans Green and Co. Ltd., London, 1966.

|13| M. D. Savage, "The Zero Pressure Gradient Condition," ASME Journal of Tribology, Vol. 107, pp. 252-255, 1985.

|14| J. C. Coyne and H. G. Elrod Jr., "Conditions for the Rupture of a Lubrication Film. Part I: Theoretical Model, ASME Journal of Lubrication Technology," Vol. 92, pp.451-456, 1970.

|15| R. H. Buckholz, "Cavitation Boundary Shapes for Submerged Short Journal Bearings Using Newtonian Lubricants," ASME Journal of Applied Mechanics, Vol. 107, pp. 267-273, 1985.

|16| R. H. Buckholz, J. Lin and C. H. T. Pan, "The Role of Axial Edge Effects and Cavitation in Lubrication for Short Journal Bearings," ASME Journal of Applied Mechanics, Vol. 107, pp. 267-273, 1985.

|17| S. V. Patankar, "Numerical Heat Transfer and Fluid Flow," Hemisphere Publishing Corporation, New York, 1980.

|18| A. T. Prata, R. T. S. Ferreira, D. E. B. Lilie and M. G. D. Bortoli, "Performance Analysis of Finite Journal Bearings under Dynamic Load Through the Integration of Reynolds Equation - Part I, "(in Portuguese) Technical Report EMBRACO-UFSC, p. 46, 1986.

|19| W. J. Minkowycz and F. M. Sparrow, editors "Numerical Heat Transfer", An International Journal of Computation and Methodology published by Hemisphere Publishing Corporation, New York, 1980.

|20| A. T. Prata, R. T. S. Ferreira, D. E. B. Lilie and M. C. D. Bortoli, "Performance Analysis of Finite Journal Bearings under Dynamic Load Through the Integration of Reynolds Equation - Part II, "(in Portuguese) Technical Report EMBRACO-UFSC, p. 66, 1986.

|21| A. T. Prata and R. T. S. Ferreira, "The Accuracy of Short Bearing Theory in Presence of Cavitation, "to appear in ASME Journal of Tribology.

|22| O. Pinkus and B. Sternlicht, "Theory of Hidrodynamic Lubrication", McGraw Hill Book Co., New York, 1961.

|23| A. T. Prata, R. T. S. Ferreira, D. E. B. Lilie and M. G. D. Bortoli, "Performance Analysis of Finite Journal Bearings under Dynamic Load Through the Integration of Reynolds Equation - Part III, "(in Portuguese) Technical Report EMBRACO-UFSC, p. 74, 1987.

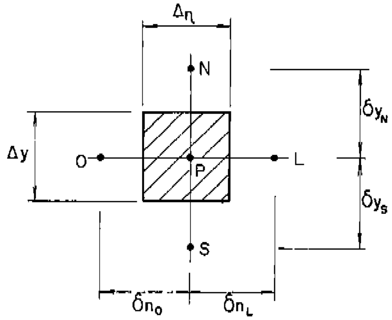

Fig. 1 - Typical control volume in the solution domain.

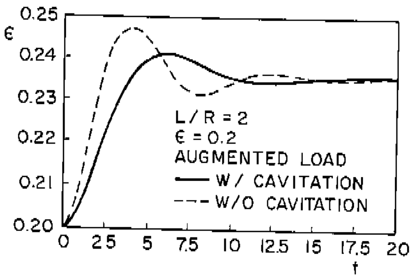

Fig. 2 - Variation of ε with time when the load is augmented

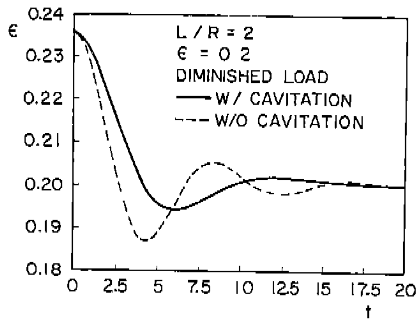

Fig. 3 - Variation of ε with time when the load is diminished

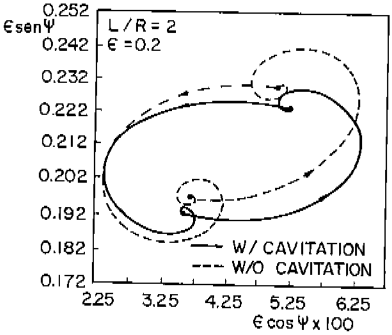

Fig. 4 - Shaft orbit for the entire cycle in which the load is augmented and diminished